Organometallic neptunium(III) complexes

Michał S. Dutkiewicz,[a,b] Joy H. Farnaby,[a, f] Christos Apostolidis,[b] Eric Colineau,[b] Olaf Walter,*[b] Nicola Magnani,[b] Michael G. Gardiner,[c] Jason B. Love,*[a] Nikolas Kaltsoyannis,*[d,e] Roberto Caciuffo,*[b] Polly L. Arnold*[a]

[a] *EaStCHEM School of Chemistry, University of Edinburgh, The King's Buildings, Edinburgh EH9 3FJ, U. K.; Tel: +44 131 6505429; Fax: +44 131 6506453; Email: Polly.Arnold@ed.ac.uk, Jason.Love@ed.ac.uk*

[b] *European Commission, Joint Research Centre (JRC), Institute for Transuranium Elements (ITU), Postfach 2340, D-76125, Karlsruhe, Germany; Email: Olaf.Walter@ec.europa.eu, Roberto.Caciuffo@ec.europa.eu*

[c] *School of Physical Sciences (Chemistry), University of Tasmania, Private Bag 75, Hobart TAS 7001, Australia.*

[d] *Department of Chemistry, University College London, 20 Gordon Street, London WC1H 0AJ, U.K.; Tel: +44 207 6794670; Fax: +44 207 6797463.*

[e] *School of Chemistry, University of Manchester, Oxford Road, Manchester M13 9PL, U.K.; Tel: +44 161 275 4692; Email: Nikolas.Kaltsoyannis@manchester.ac.uk*

[f] *Current address: Department of Chemistry, Imperial College London, South Kensington Campus, SW7 2AZ, U.K.*

Abstract

Studies of transuranic organometallic complexes provide particularly valuable insight into covalent contributions to the metal-ligand bonding, in which the subtle differences between the transuranium An^{III} ions and their lighter lanthanide Ln^{III} counterparts are of fundamental importance for effective remediation of nuclear waste. Unlike the organometallic chemistry of uranium, which has focused strongly on U^{III} with spectacular advances, that of the transuranics is significantly technically more challenging and has remained dormant. In the case of neptunium, it is limited mainly to Np^{IV}. Here we report a range of new Np^{III} organometallics, and characterize their molecular and electronic structures. These studies suggest that the lower oxidation state of Np^{II} complex is chemically accessible, and that Np^{III} complexes could act as single molecule magnets. Significant d- and f-electron contributions to key Np^{III} orbitals are found in comparison with lanthanide analogues, showing that fundamental Np organometallic chemistry can provide new insight into f-element behaviour.

Studies of transuranic organometallic complexes with aromatic π-electron systems are particularly valuable to the understanding of the bonding, and physical and chemical properties of the actinides because they give insight into covalent contributions to the metal-ligand bonding[1]. The heavier, radiotoxic actinide elements exist primarily in the +3 oxidation state, and hence their chemical separation from Ln^{III} ions in nuclear waste is very difficult. The selectivity of the best available An^{III} extractants is attributed to subtly higher bonding covalency, but is not well understood and theory cannot yet make predictions. Unlike the organometallic chemistry of uranium, which has focused strongly on U^{III} and seen spectacular advances[2-4], that of the transuranics has remained dormant and, in the case of neptunium, is limited mainly to Np^{IV}. The only known organometallic compounds of neptunium, the first transuranic element, are a handful of cyclopentadienyl complexes [Cp_3NpX] (Cp = (Cp = *cyclo*-pentadiene anion, X = Cp, Cl, OMe, *n*-Bu, Ph)[5-7], and the cyclooctatetraenyl sandwich [$Np(COT)_2$] (COT = *cyclo*-octatetraene dianion)[8]. These compounds were milestones in helping understand actinide bonding, and [$Np(COT)_2$] shows fascinating

magnetic bistability[9]. Analyses now standard in organometallic chemistry such as single crystal X-ray structures were determined for only a few Np^{IV} complexes, and ^1H NMR spectroscopic data reported in just a couple of cases. While exploratory reductions to the Np^{III} oxidation state afforded powders presumed to be solvated $Np^{III}Cp_3$ and $K[Np(COT)_2]$ respectively, only scant spectroscopic data, and no structural data exist for any organometallic Np^{III} complex[10,11]. The severe radiotoxicity of Np, the accessibility of its radionuclides, and the requirements to work with small sample sizes compound the traditional difficulties associated with handling air-sensitive, highly paramagnetic organometallic early actinide complexes.

Single arene - f-block π- and δ-(back)bonding interactions have been used for C-H bond functionalisation[12], and to stabilise the unusually low formal oxidation state of U^{II} [13], while bis(arene) sandwich molecules have been made for all areas of the periodic table except the actinides, where only predictions of stability exist[14]. A desire to better understand the subtlest actinide π- and δ-symmetry bonding interactions has led us to the flexible macrocycle H_2L^{Ar} *trans*-calix[2]benzene[2]pyrrole[15], which can geometrically and electronically mimic two cyclopentadienyl ions i.e. bis(η^5-pyrrolyl), or a bis(η^6-arene) sandwich form[16]. Hybrid density functional theory (DFT) calculations found significant covalent bonding in both binding modes in the di-U^{III} adduct[16]. We have also used non-aqueous Np^{III} iodides[17] to make magnetically coupled U^{III} and Np^{III} complexes that we could not structurally characterise[18]. We here report our successful attempts to demonstrate that organometallic ligands other than the cyclopentadienyl anion, i.e. $(L^{Ar})^{2-}$, can support a range of organometallic neptunium(III) complexes, and explore their redox chemistry and molecular and electronic structure and bonding.

Results and Discussion

Synthesis and redox chemistry

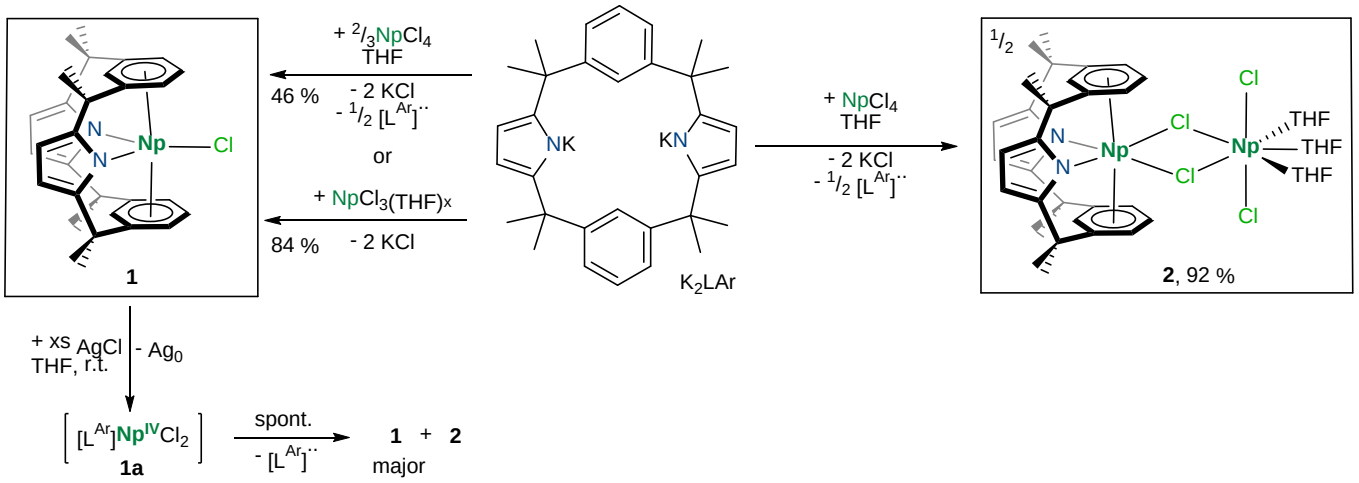

Figure 1 Synthesis of mono and dinuclear bis(arene)-bound Np(III) L^{Ar} complexes 1 and 2 from the spontaneous reduction of the Np^{IV} starting material. Oxidation of **1** with silver chloride produces maroon-coloured solutions consistent with $[Np^{IV}(L^{Ar})Cl_2]$ (**1a**) that gradually revert back to **1** and **2** over time.

The reaction between $^{237}NpCl_4$ and 1.5 equivs of dipotassium K_2L^{Ar} affords the dark-red, crystalline, mononuclear Np^{III} complex $[(L^{Ar})^{237}NpCl]$ **1** in 46 % yield (theor. 50 %) (Figure 1), or in 84 % yield from the equimolar reaction between *in situ* generated $^{237}NpCl_3(THF)_x$ and K_2L^{Ar} in THF (tetrahydrofuran) at room temperature. Interestingly, the equimolar reaction between $^{237}NpCl_4$ and K_2L^{Ar} yields the dark red crystalline dinuclear Np^{III} complex $[(L^{Ar})^{237}Np_2Cl_4(THF)_3]$ **2** in 92 % yield. The ^1H and ^{13}C NMR spectra of **1** show C_{2v} symmetry; the resonances are broadened and shifted due to the paramagnetic Np^{III} $5f^4$ ion, but assignable, proving that multinuclear NMR solution spectroscopy of organometallic Np^{III} is a useful analytical tool[19].

Given that all previous organometallic chemistry of Np^{IV} salts has retained the Np^{IV} oxidation state, the spontaneous reduction to Np^{III} provides an excellent entry into organo-Np^{III} chemistry that avoids additional procedures with reductants such as potassium metal that were required in the previous

explorations. We account for the reduction by considering the ability of the flexible L^{Ar} to bind in a κ^1-configuration, in contrast to the cyclopentadienyl anion that rarely diverts from η^5-coordination. This can allow a Np-L bond homolysis to occur, providing a reducing electron to Np and releasing the ligand as a radical. The use of coordinating THF in these reactions may have enabled the further substitution of chloride by $(L^{Ar})^{2-}$ in a κ^1-pyrrolide coordination mode. This is consistent with the yields and by-products, and the recent report of a decomposition product in $Sm^{III}(L^{Ar})$ chemistry; $[(L^{Ar})(HL^{Ar'})SmCl]$ contains one κ^1-bound $(HL^{Ar})^{1-}$ equivalent [20].

Single crystals of **1** and **2** were analysed by X-ray crystallography; the molecular structures (Figure 2a,b) confirm the same η^6-arene:κ^1-pyrrolide binding mode to Np^{III} that was observed for the isotypic Sm^{III} and U^{III} complexes. These are the first instances of the bis(arene) sandwich motif in a transuranic complex; **2** formally contains an additional equivalent of $NpCl_3(THF)_3$ through chloride-bridging. In the bis(η-arene) structures of **1** and **2** the Np-arene centroids are 2.601 Å in **1** and average 2.63 Å in **2**, with further ligand interactions made with Np-N bond distances of 2.447(2) Å in **1** and 2.486(5), 2.496(6) Å in **2**. The Cnt_{Ar}-Np-Cnt_{Ar} angles, 174.20(4)° in **1** and 173.2(1)° in **2**, are close to linear and similar to that found in the isotypic series $[(L^{Ar})UX]$ (four examples, range 173.4(3)–174.4(2)°) and $[(L^{Ar})SmCl]$ (175.95(8)°). The mean Np-C_{Ar} separations in both **1** (2.95 Å) and **2** (3.01 and 2.96 Å) are remarkably similar to those in the isostructural $[(L^{Ar})UI]$ (range 2.95–2.98 Å) and $[(L^{Ar})SmCl]$ (2.98 Å). The difference in M-Cl bond distances between **1** and $[(L^{Ar})SmCl]$ is the same within standard uncertainties once normalised for the Sm^{III} and Np^{III} radii[21], and longer than in Np^{IV} complexes[22,23]. Figure 2c shows the molecular structure of complex **3**, described below, which represents the first structural characterisation of a metallocene-type geometry for a Np^{III} centre.

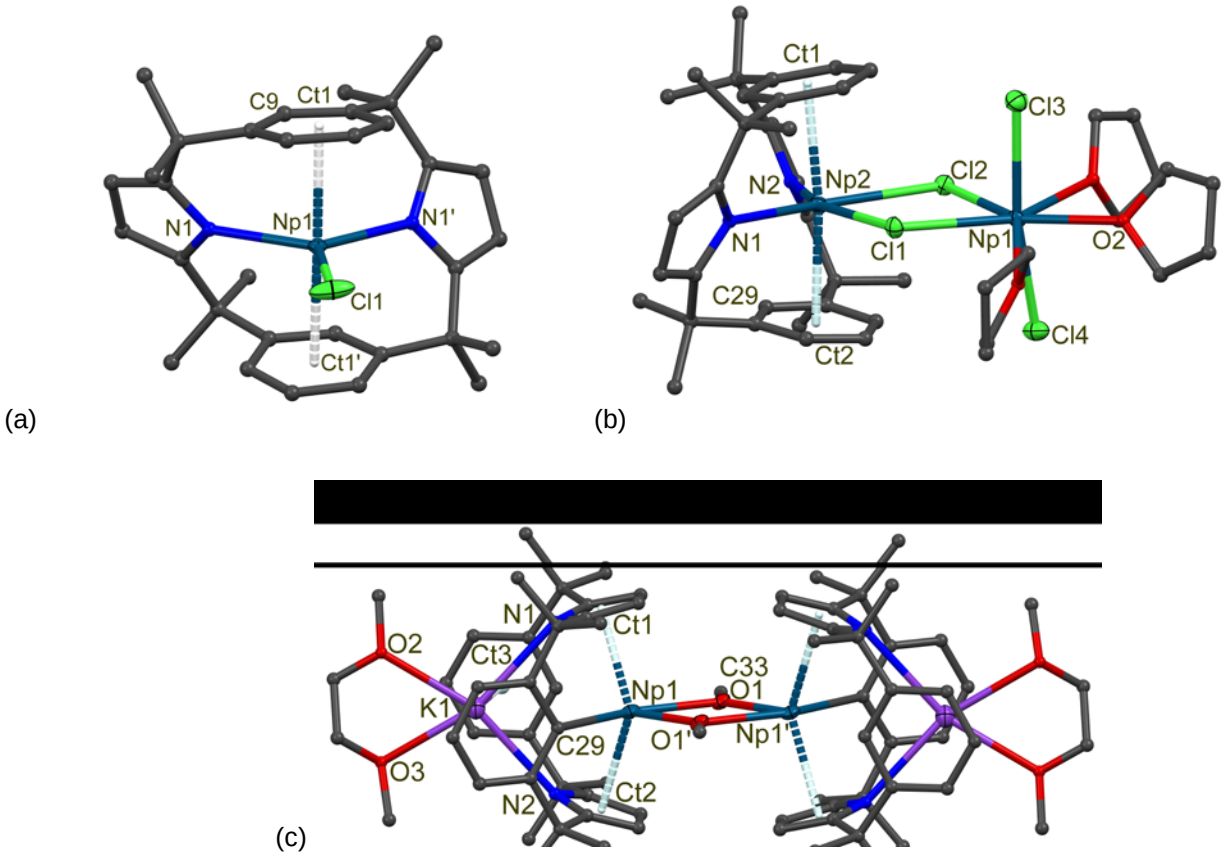

Figure 2. The molecular structures of the three organometallic Np^{III} complexes confirming the first bis(arene) sandwich coordination motif for a transuranic ion and the first structural characterisation of a metallocene-type geometry for a Np^{III} centre: (a) $[(L^{Ar})NpCl]$ 1, (b) $[(L^{Ar})Np_2Cl_4(THF)_3]$ 2 and (c) $[K(dme)(L^{Ar-H})Np(OMe)]_2$ 3. Complex **1** is drawn face-on to show the bis(η^6-arene) sandwich coordination geometry while complex **3** (see below for synthesis) is drawn side-on to show the switch to the bis(η^5-pyrrolide) coordination geometry. A potassium counter-cation resides in the other pocket of the ligand in **3**. Displacement ellipsoids are drawn at 50 % probability, ligand framework and coordinated solvents drawn as capped sticks, hydrogen atoms and lattice solvent are omitted for clarity. Selected distances (Å) and angles (°) for **1**: Np1-Cl1 2.6694(9), Np1-N1 2.447(2), Np1-C_{aryl} range 2.853(2) to 3.010(3), Ct1-Np1-Ct1' 174.20(4); For **2**: Np1-Cl1 2.814(2), Np2-Cl1 2.864(2), Np2-N1 2.496(6), Np2-C_{aryl} range 2.854(6) to 3.022(6), Ct1-Np2-Ct2 173.2(1); For **3**: Np1-O1 2.288(9), Np1-C29 2.660(13), Np1-C_{pyrr} range 2.757(12) to 2.998(11), K1-C_{aryl} range 3.051(13) to 3.366(15), Ct1-Np1-Ct2 143.98(15).

Given the strong stabilisation afforded to Np^{III} by $(L^{Ar})^{2-}$, and recent landmark syntheses of formally Th^{II} and U^{II} complexes[13,24], we added the reductant NaK_3 to a 1,2-dimethoxyethane (dme) solution of **1**, which turned purple black, and precipitated KCl, Figure 3a. The Vis-nIR spectrum of the supernatant (Figure

3b) has broad absorptions with extinction coefficients centred around 600 nm and 1275 nm, characteristic of *d* - *f* and *d* - π^* transitions and suggestive of the formation of the new formal oxidation state Np^{II} in the neutral, arene-stabilised complex [(L^{Ar})Np^{II}(dme)] **3a**. In contrast, higher oxidation state neptunium complexes have sharp transitions in the nIR region consistent with forbidden *f-f* transitions; the Vis-nIR of **1** (Supplementary Figure S5) displays line-like absorptions with the low extinction coefficients (ε of the order of tens) expected for *f* - *f* transitions. Similar changes upon reduction of 6π-organometallic complexes have been seen for [K(2.2.2-cryptand)][(η-$C_5H_4SiMe_3)_3$M] (M = Ln, U)[25] with the appearance of an absorption at 600 nm for M = U (ε = 750 M^{-1} cm^{-1}), and [K(2.2.2-cryptand)][Th{η^5-$C_5H_3(SiMe_3)_2$-1,3}$_3$][26] at 650 nm (ε = 23000 M^{-1} cm^{-1}). The putative Np^{II} complex **3a** is not stable in solution, and lightens in color to reddish-brown over 12 hours; the strongly absorbing Vis-nIR bands of **3a** are replaced by new and weak absorptions in the region 780-1350 nm assigned to the new Np^{III} complex [K(dme)$_n${(L^{Ar})Np^{II}(OCH_3)}]$_2$ **3** (Figure 3). Control reactions also support the assignment of the reducing electron being based on the metal rather than the ligand: The UVvis spectra of dme solutions of the dipotassium salt [K_2L^{Ar}] treated with NaK_3 contain a single broad band at 716 nm, the same as that of the solvated electron formed on contacting NaK_3 with dme, that decay within minutes (Supplementary figure S8). All attempts (unpublished work) to reduce analogous thorium(IV)(L^{Ar}) complexes have been unsuccessful; the reduction potential of Th^{IV} is usually estimated as around -3V, so ligand reduction would be anticipated where possible in organo-thorium chemistry. TD-DFT calculations on the reduction product were not pursued owing to the intrinsic unreliability of the approach for a system with five unpaired 5f electrons and (most likely) highly multiconfigurational excited states. Notably, solutions of **3a** stored over NaK_3 remain purple-black indefinitely, giving further weight to the capability of the ligand to support Np^{II} under maintained reducing conditions. Small, black plate-shaped crystals of **3a** isolated from these solutions gave only weak diffraction.

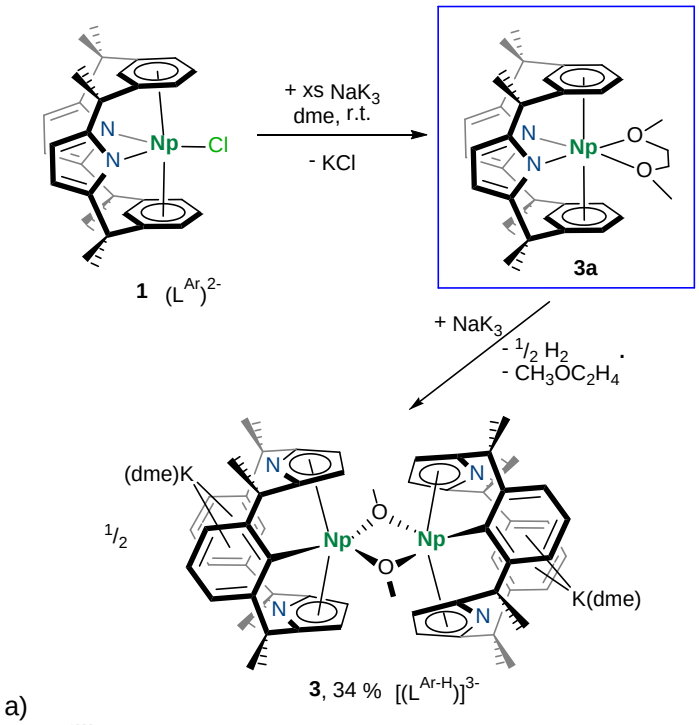

a)

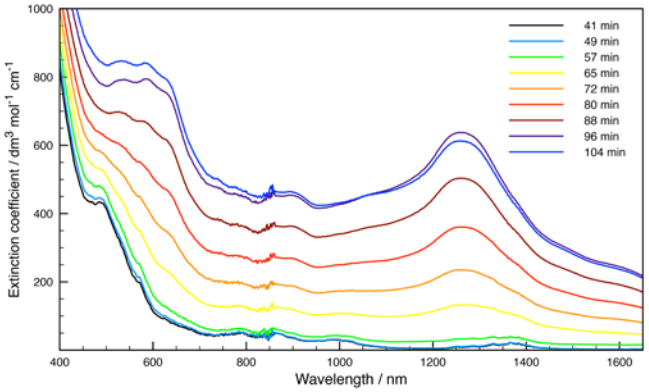

b)

Figure 3. a) Reduction of 1 with NaK_3 produces near-black solutions consistent with the formation of the new [$Np^{II}(L^{Ar})$(dme)] 3a. The complex is thermally unstable and gradually converts to the metalated $(L^{Ar})^{3-}$ Np^{III} aryl complex $[K(dme)_n\{(L^{Ar})Np^{II}(OCH_3)\}]_2$ **3** in which the L^{Ar} ligand adopts a metallocene-type geometry for the new Np^{III} centre. **b) The Vis-NIR spectra of dme solutions of 1 and NaK_3 recorded over time show the formation of 3a at 19 °C**; the strong absorptions growing in around 600 nm and 1275 nm (see legend for time period between addition of reductant and recording of spectrum) bleach on transformation to **3** when the isolated sample is stored at ambient temperature in the absence of reducing agent (^{237}Np concentration 0.56 mM).

The identity of **3** was confirmed by single crystal X-ray diffraction (Figure 2c above). The ligand is triply deprotonated as a result of the metalation of one arene $(L^{Ar\text{-}H})^{3-}$, and the $[Np^{III}(OMe)]$ moiety is now bound in the 'metallocene-type' geometry provided by the two η^5-bound pyrrolide groups [16]. A dimer is formed through asymmetric methoxide bridging which has presumably arisen from the cleavage of dme. The shorter of the two Np-O bond lengths, 2.296(8) Å, is longer than the Np^{IV}–OPh bond of 2.137(7) Å in $Cp_3Np(OPh)$[27]. This O-C bond cleavage is common for reduced electropositive metal complexes, and supports the assignment of a reactive Np^{II} centre in **3a**. We have previously observed the double

metalation of L^{Ar} from the treatment of $Th^{IV}(L^{Ar})$ complexes with either reductants or non-nucleophilic bases[16], but the only occasion on which we have observed a An^{3+} cation to reside in the cavity provided by the two pyrrolides (rather than the two arenes) is in the di-U^{III} adduct, $U^{III}_2I_4(L^{Ar})$[16]. In this latter case, the ligand undergoes a significant strain-energy penalty from the incorporation of two metal cations.

Magnetic behaviour

We were curious as to whether the mononuclear neptunium(III) complex **1** could function as a single molecule magnet (SMM), i.e. exhibit slow relaxation of the magnetisation at low temperatures. Actinide metal cations offer an alternative SMM design approach by combining the best properties of 3d (sizeable exchange interaction)[28] and 4f (large single-ion anisotropy) magnetic ions[29], and it has even been suggested that all U^{III} complexes should possess inherent SMM character[30,31]. The imaginary part of the ac magnetic susceptibility of **1** is very small with respect to χ_{dc} (Figure 4); however, a significant increase below 10 K is clearly observed and may be attributed to a slowing down of the magnetization dynamics. This signifies that the onset of SMM behaviour should occur at temperatures lower than we can measure, i.e. 2 K.

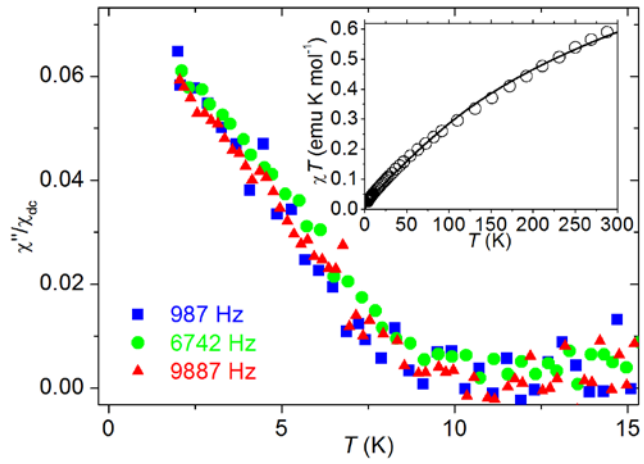

Figure 4. Ratio between the imaginary part of the ac magnetic susceptibility and the static (dc) susceptibility measured for [(L^{Ar})NpCl] (1) as a function of temperature and for different frequencies. Regardless of frequency (see color legend), at around 10K the direction of magnetisation of the sample can no longer keep up with the alternating magnetic field applied by the magnetometer, as the magnetic relaxation begins

to slow down. Inset: temperature (T) dependence of the dc magnetic susceptibility χ of (**1**) plotted as χT vs T (open dots: experimental data measured with a magnetic field of 1 T, line: ligand-field calculation).

Computational bonding analysis

Complex **1**, the 4f Sm^{III} complex $[SmCl(L^{Ar})]$[20] and our 5f U^{III} systems provide the first opportunity to explore and validate the bonding in an isostructural set of f-block organometallics featuring a transuranic element. DFT quantum chemical calculations were therefore undertaken on **1c-MCl** (M = Sm, U, Np), **1c-SmI** and **1c-NpI**. We have previously described the valence electronic structure of **1c-UI** in detail[16]. For all six systems, modest and consistent metal d orbital contributions are found to the M-N and M-arene bonding, the latter being about half of that in a comparable transition metal bonding situation. By contrast, the M-halogen bonding orbitals show much larger variations in covalency, with significant increases in metal d (in M-X σ) and metal f (in M-X π for **1c-MI**) from Sm to U and Np.

By contrast to the primarily ligand-localised valence MOs, the canonical valence molecular orbital (MO) energy level diagrams for the α spin orbitals of the three **1c-MI** complexes show there is significant variation in the energies of the metal f-based orbitals (Figure 5). In **1c-UI**, the three 5f electrons are the least stable, while in **1c-NpI** the four, singly occupied 5f-based orbitals drop below the highest occupied pyrrolide levels. In **1c-SmI**, the 4f-based orbitals are significantly more stable than any of the other valence orbitals considered. In keeping with the traditional picture of the bonding in lanthanide and actinide systems[32], the almost core-like 4f orbitals of Sm^{III} are too low in energy and radially contracted to participate in bonding, while the 5f orbitals of the early actinides have greater radial extension and sufficiently higher energies to enable metal-ligand orbital overlap. Hence, although the bonding in f element molecules is predominantly ionic, the early actinides can form more covalent bonds than their lanthanide analogues.

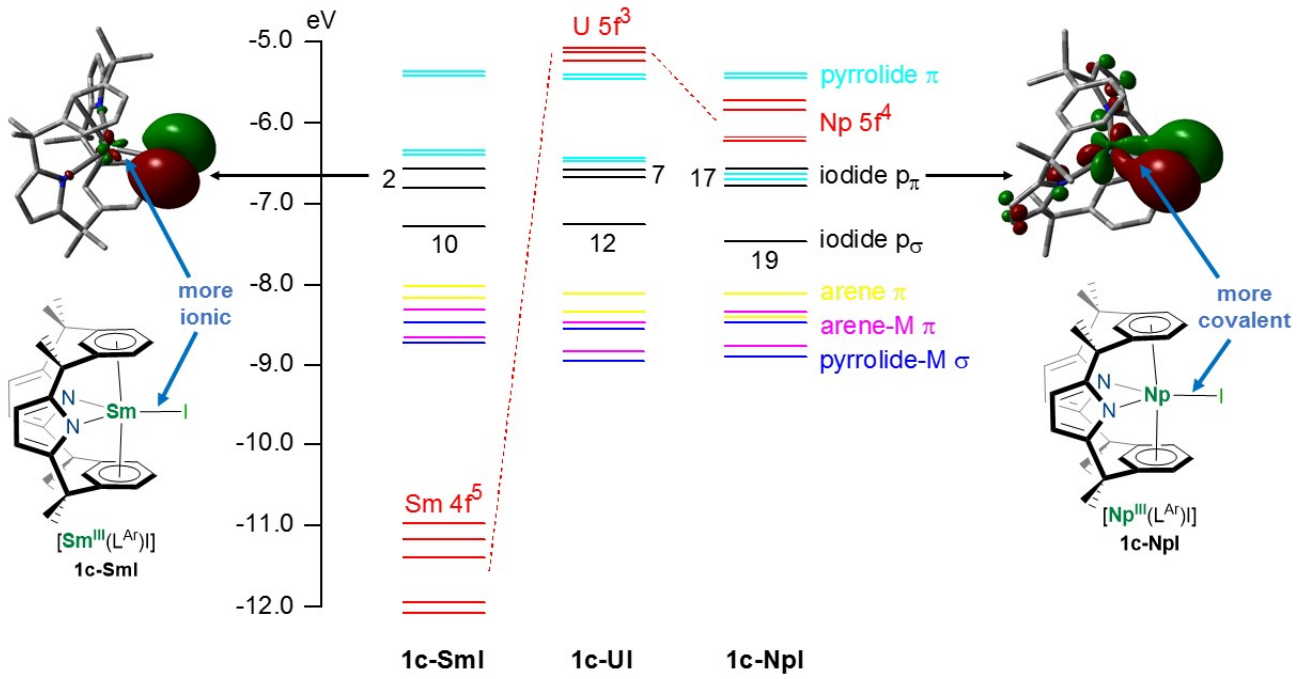

Figure 5. Molecular orbital (MO) diagrams for 1c-MI (M = Sm, U, Np). Horizontal lines represent the energies of the α-spin MOs (in electronvolts, eV), and their principal character is indicated by the line and text colour: cyan = pyrrolide–π, black = iodide-p, yellow = arene-π, magenta = arene-M π, blue = pyrrolide-M σ, red = metal-f. The number of solid red lines indicates the number of electrons of predominant metal f character; $4f^5$ (Sm), $5f^3$ (U), $5f^4$ (Np). The dashed red lines highlight the dramatic change in energy as a function of metal. The black numbers beside the iodide p_π and p_π-based MOs indicate their total metal atomic orbital content (%),highlighting the substantial increases in metal contribution from Sm-U-Np. The image on the right is an iodide p_π-based MO of **1c-NpI**, containing a 17 % Np 5f covalent contribution (H omitted for clarity, MO isosurface value = 0.035). Red and green indicate the MO phases. The image on the left is the analogous MO for **1c-SmI**; it contains almost no metal 4f contribution (2 %), indicating an ionic interaction. MOs lying between the pyrrolide-M σ and 4f levels in energy in **1c-SmI** are omitted. Data for **1c-UI** from the literature.[16]

The deviations of metal spin densities from the values expected for formal oxidation states can provide a measure of covalency[33,34]. Here, Hirshfeld, Mulliken and Quantum Theory of Atoms-in-Molecules (QTAIM) calculations show small deviations which have been explored further by examination of the metal contributions to key valence MOs (Extended Data Table 3). In **1c-MI**, the principal character of these MOs is generally unambiguous, although more delocalisation is present in **1c-MCl**. The metal

content of the metal-arene π bonding orbitals is remarkably similar in all six target systems (6 to 8 %) and is largely d-based, in agreement with that proposed for the hypothetical $U(C_6H_6)_2$[14]. These values are about half that in the classical d-block $W(\eta^6\text{-}C_6H_6)_2$, which we calculate to have 16 % metal 5d character in the e_{1g} metal-ring π bonding orbitals. By contrast to the M-arene π orbitals, only the metal f orbitals contribute to the halogen pπ-based MOs, with significant variation across the metals; the f character is almost negligible (around 3 %) in all the metal chlorides **1c-MCl** and **1c-SmI** but rises sharply through **1c-UI** to 17 % 5f in **1c-NpI**. The principal metal contributor to the M-X σ bonding MOs is d in all cases bar **1c-NpI**, and there is generally more metal content in these MOs than in the π type levels. As with the latter, there is a significant (19 %, of which 8 % d and 11 % f) metal contribution to the Np-I σ bonding orbital in **1c-NpI**.

It is increasingly recognised that metal-ligand covalency may be either *energy*-driven or *overlap*-driven, or potentially a combination of both[35]. The former arises when atomic orbitals on metal and ligand have very similar energies but little spatial overlap, while the latter involves significant orbital overlap. The QTAIM, an electron density-based approach that we have employed extensively to study covalency in the f block[36], provides us with a means to distinguish these covalency mechanisms; overlap-driven covalency should be accompanied by an increase in the electron density in the internuclear bonding region, while energy-driven covalency should not. We were therefore keen to establish if the differences in the metal-halogen orbital compositions seen within the present organometallic systems are mirrored by the QTAIM metrics, particularly in light of our previous studies of other organo f element systems which have shown the orbital composition and QTAIM data to paint contrasting pictures[34]. The absolute values of the M-X bond critical point electron (ρ) and energy densities (H) are small (Extended Data Table 4), indicating largely ionic bonds at the QTAIM level. That said, and in agreement with the increasing metal contributions to the M-X bonding MOs, there are increases in both ρ and H from Sm to U and Np for a given halogen, and in delocalisation indices (a QTAIM measure of bond order, Extended Data Table 4) from the lanthanide to the actinides. This shows that the covalency explanation presented here for the neptunium iodide arises from a spatial overlap of the orbitals, rather than from accidental energy

degeneracy.

Collectively, these results show a range of unanticipated behaviours, both chemically and electronically, for the Np(III) ion in an organometallic environment. The new redox chemistry, unusual magnetic behaviour and covalency in the bonding that we have been able to explore compensates for the additional complexity of handling this radionuclide, and should open up new vistas in anaerobic neptunium science.

Methods

Caution! Compounds of the ^{237}Np isotope represents a potential health risk owing to α emission (4.958 MeV, $t_{1/2}$ = 2.14×10^6 years, a = 0.7 mCi g^{-1}) and its decay to ^{233}Pa which is a potent β emitter (0.570 MeV, $t_{1/2}$ = 26.97 days, a = 21 kCi g^{-1}). Handling of the ^{237}Np radioisotope should be undertaken in a properly regulated and controlled radiological facility, in this case in the radiochemical laboratories at the Joint Research Centre (JRC) – Institute of Transuranium Elements (ITU). Unsealed radioactive compounds were manipulated in dinitrogen filled (99+ %), negative-pressure radiological gloveboxes containing a separate high-vacuum/argon double manifold which could be used to maintain a positive pressure of inert gas during the handling of reagents and solutions with more standard Schlenk techniques. A UV-Vis-nIR optical chamber and an ATR-IR spectrometer were contained within radiological gloveboxes to enable direct measurements. NMR spectra were recorded promptly on solutions in fluoropolymer NMR tube liners (degassed at 140 °C, 6×10^{-4} mbar, 12 h) inserted into a standard borosilicate glass NMR tube placed in a PVC bag, which was sealed by welding. In spite of the drying/degassing precautions, the Np^{III} samples show evidence of reaction with the inert liners over the course of a day.

Syntheses of the complexes were carried out in Teflon tap-equipped glass ampoules between the appropriate amount of Np^{IV} (or *in situ*-generated Np^{III}) chloride and dipotassium salt of the ligand L^{Ar} in a suitable dry, and oxygen-free aprotic solvent. Work-up of the solutions afforded the target complexes as powders or crystalline materials which were fully characterised by a suite of NMR, IR, UVVis-nIR spectroscopies, SQUID magnetometry and single crystal X-ray diffraction where possible. *In-situ* oxidations or reductions were carried out respectively by addition of AgCl or K or NaK_3 alloy to THF or dme solutions of complexes. Density functional theory and atoms-in-molecules computational analyses were carried out on the mononuclear complexes complex $[(L^{Ar})M^{III}Cl]$ for M = Sm, U, and Np after confirmation that the computed molecular geometries were in excellent agreement with the available experimental data.

Full descriptions of the methods, as well as additional tables (4) and figures (10), are given in the Supplementary Information.

References:

1 Nash, K., Madic, C., Mathur, J. N. & Lacquement, J. in *The Chemistry of the Actinide and Transactinide Elements* Vol. 5 (eds Joseph J. Katz, Lester R. Morss, Norman M. Edelstein, & Jean Fuger) Ch. 24, 2622-2798 (Springer, 2010).

2 LaPierre, H. S. & Meyer, K. Activation of small molecules by molecular uranium complexes. *Progr. Inorg. Chem.* **58**, 303-416 (2014).

3 Liddle, S. T. The renaissance of non-aqueous uranium chemistry. *Angew. Chem. Int. Ed.* **54**, 8604-8641 (2015).

4 Arnold, P. L., McMullon, M. W., Rieb, J. & Kuhn, F. E. C-H bond activation by f-block complexes. *Angew. Chem. Int. Ed.* **54**, 82-100 (2015).

5 Fischer, E. O., Laubereau, P., Baumgärtner, F. & Kanellakopulos, B. Tricyclopentadienylneptunium-chlorid. *J. Organomet. Chem.* **5**, 583-584 (1966).

6 Baumgärtner, F., Fischer, E. O., Kanellakopulos, B. & Laubereau, P. Tetrakis(cyclopentadienyl)neptunium(IV). *Angew. Chem.* **80**, 661-661 (1968).

7 Bohlander, R. *The organometallic chemistry of neptunium*, Kernforschungszentrum Karlsruhe G.m.b.H. (Germany, F.R.). Inst. fuer Heisse Chemie; Karlsruhe Univ. (T.H.) (Germany, F.R.). Fakultaet fuer Chemie, (1986).

8 De Ridder, D. J. A., Rebizant, J., Apostolidis, C., Kanellakopulos, B. & Dornberger, E. Bis(cyclooctatetraenyl)neptunium(IV). *Acta Cryst. C* **52**, 597-600 (1996).

9 Magnani, N. *et al*. Magnetic memory effect in a transuranic mononuclear complex. *Angew. Chem. Int. Ed.* **50**, 1696-1698 (2011).

10 Eisenberg, D. C., Streitwieser, A. & Kot, W. K. Electron transfer in organouranium and transuranium systems. *Inorg. Chem.* **29**, 10-14 (1990).

11 Burns, C. & Eisen, M. in *The Chemistry of the Actinide and Transactinide Elements* Vol. 5 (eds Joseph J. Katz, Lester R. Morss, Norman M. Edelstein, & Jean Fuger) Ch. 25, 2799-2910 (Springer, 2010).

12 Arnold, P. L., Mansell, S. M., Maron, L. & McKay, D. Spontaneous reduction and C-H borylation of arenes mediated by uranium(III) disproportionation. *Nat. Chem.* **4**, 668-674 (2012).

13 La Pierre, H. S., Scheurer, A., Heinemann, F. W., Hieringer, W. & Meyer, K. Synthesis and characterization of a uranium(II) monoarene complex supported by δ backbonding. *Angew. Chem. Int. Ed.* **53**, 7158-7162 (2014).

14 Hong, G., Schautz, F. & Dolg, M. Ab initio study of metal−ring bonding in the bis(η^6-benzene)lanthanide and -actinide complexes $M(C_6H_6)_2$ (M = La, Ce, Nd, Gd, Tb, Lu, Th, U). *J. Am. Chem. Soc.* **121**, 1502-1512 (1999).

15 Sessler, J. L., Cho, W.-S., Lynch, V. & Král, V. Missing-link macrocycles: hybrid heterocalixarene analogues formed from several different building blocks. *Chem. Eur. J.* **8**, 1134-1143 (2002).

16 Arnold, P. L. *et al*. Switchable π-coordination and C-H metallation in small-cavity macrocyclic uranium and thorium complexes. *Chem. Sci.* **5**, 756-765 (2014).

17 Avens, L. R. *et al*. A convenient entry into trivalent actinide chemistry: synthesis and characterization of $AnI_3(THF)_4$ and $An[N(SiMe_3)_2]_3$ (An = U, Np, Pu). *Inorg. Chem.* **33**, 2248-2256 (1994).

18 Arnold, P. L. *et al*. Synthesis of bimetallic uranium and neptunium complexes of a binucleating macrocycle and determination of the solid-state structure by magnetic analysis. *Inorg. Chem.* **49**, 5341-5343 (2010).

19 Bursten, B. E., Rhodes, L. F. & Strittmatter, R. J. The bonding in tris(η^5-cyclopentadienyl)actinide complexes. IV: electronic structural effects in $AnCl_3$ and $(\eta^5\text{-}C_5H_5)_3$ An (An = thorium-californium) complexes. *J. Less-Common Met.* **149**, 207-211 (1989).

20 Ilango, S., Vidjayacoumar, B. & Gambarotta, S. Samarium complexes of a σ-/π-pyrrolide/arene based macrocyclic ligand. *Dalton Trans.* **39**, 6853-6857 (2010).

21 Shannon, R. D. Revised effective ionic-radii and systematic studies of interatomic distances in halides and chalcogenides. *Acta Cryst. A* **32**, 751-767 (1976).

22 Minasian, S. G. *et al*. Synthesis and Structure of $(Ph_4P)_2MCl_6$ (M = Ti, Zr, Hf, Th, U, Np, Pu). *Inorg. Chem.* **51**, 5728-5736 (2012).

23 Bagnall, K. W., Payne, G. F., Alcock, N. W., Flanders, D. J. & Brown, D. Actinide structural studies. Part 8. Some new oxygen-donor complexes of trichloro(cyclopentadienyl)neptunium(IV); the crystal structure of trichloro(η^5-cyclopentadienyl)bis(methyldiphenylphosphine oxide)neptunium(IV). *Dalton Trans.*, 783-787 (1986).

24 Langeslay, R. R., Fieser, M. E., Ziller, J. W., Furche, F. & Evans, W. J. Synthesis, structure, and reactivity of crystalline molecular complexes of the $\{[C_5H_3(SiMe_3)_2]_3Th\}^{1-}$ anion containing thorium in the formal +2 oxidation state. *Chem. Sci.* **6**, 517-521 (2015).

25 MacDonald, M. R. *et al*. Identification of the +2 oxidation state for uranium in a crystalline molecular complex, [K(2.2.2-Cryptand)][$(C_5H_4SiMe_3)_3U$]. *J. Am. Chem. Soc.* **135**, 13310-13313 (2013).

26 Blake, P. C., Lappert, M. F., Atwood, J. L. & Zhang, H. The synthesis and characterisation, including X-ray diffraction study, of [Th{η-$C_5H_3(SiMe_3)_2\}_3$]; the first thorium(III) crystal structure. *Chem. Comm.*, 1148-1149 (1986).

27 De Ridder, D. J. A., Apostolidis, C., Rebizant, J., Kanellakopulos, B. & Maier, R. Tris(η^5-cyclopentadienyl)phenolatoneptunium(IV). *Acta Cryst. C* **52**, 1436-1438 (1996).

28 Arnold, P. L. *et al*. Strongly coupled binuclear uranium–oxo complexes from uranyl oxo rearrangement and reductive silylation. *Nature Chem.* **4**, 221-227 (2012).

29 Meihaus, K. R. & Long, J. R. Actinide-based single-molecule magnets. *Dalton Trans.* **44**, 2517-2528 (2015).

30 Rinehart, J. D. & Long, J. R. Exploiting single-ion anisotropy in the design of f-element single-molecule magnets. *Chem. Sci.* **2**, 2078-2085 (2011).

31 Moro, F., Mills, D. P., Liddle, S. T. & van Slageren, J. The inherent single-molecule magnet character of trivalent uranium. *Angew. Chem., Int. Ed.* **52**, 3430-3433 (2013).

32 Kaltsoyannis, N. & Scott, P. *The f elements*. (OU Press, 1999).

33 Prodan, I. D., Scuseria, G. E. & Martin, R. L. Covalency in the actinide dioxides: Systematic study of the electronic properties using screened hybrid density functional theory. *Phys. Rev. B* **76**, 033101 (2007).

34 Kirker, I. & Kaltsoyannis, N. Does covalency really increase across the 5f series? A comparison of molecular orbital, natural population, spin and electron density analyses of $AnCp_3$ (An = Th-Cm; Cp = $\eta^5\text{-}C_5H_5$). *Dalton Trans.* **40**, 124-131 (2011).

35 Neidig, M. L., Clark, D. L. & Martin, R. L. Covalency in f-element complexes. *Coord. Chem. Rev.* **257**, 394-406 (2013).

36 Huang, Q.-R., Kingham, J. R. & Kaltsoyannis, N. The strength of actinide-element bonds from the quantum theory of atoms-in-molecules. *Dalton Trans.* **44**, 2554-2566 (2015).

Supplementary Information is linked to the online version of the paper at www.nature.com/nature.

Acknowledgements Experiments were supported by the European FP7 TALISMAN project, under contract with the European Commission, the JRC ITU USERLAB programme, the University of Edinburgh, EU COST action CM1006, and the EPSRC. MSD acknowledges the European Commission

for support in the frame of the Training and Mobility of Researchers programme. We thank Dr G. Nichol for help with the X-ray crystallography. We thank Dr A. Morgenstern for help with data collection, and the Organometallic Chemistry Laboratory, CENT, University of Warsaw for additional data collection. NK thanks the UCL High Performance Computing Facility (Legion@UCL) and associated support services.

Author Contributions MSD synthesised and purified the compounds and collected and analysed synthetic data; JHF provided ligand samples and analysed synthetic data; CA collected and analysed synthetic data; EC collected and analysed magnetic data; OW collected and analysed crystallographic data; NM analysed magnetic data; MGG provided ligand samples; JBL designed the study, analysed the data, and wrote the manuscript; NK designed the computational study, carried out and analysed the calculations and wrote the manuscript; RC designed the study, analysed the data, and wrote the manuscript; PLA designed the study, analysed the data, and wrote the manuscript.

Author Information Crystallographic CIF files for the reported X-ray crystal structures are registered with the CCDC under codes 1423267-1423269. Reprints and permissions information is available at www.nature.com/reprints". The authors have no competing financial interests to declare. Correspondence and requests for materials should be addressed to Polly.Arnold@ed.ac.uk.